

When Robots Say No: The Empathic Ethical Disobedience Benchmark

Preprint

Dmytro Kuzmenko

kuzmenko@ukma.edu.ua

National University of Kyiv-Mohyla Academy
Kyiv, Ukraine

Nadiya Shvai

National University of Kyiv-Mohyla Academy

Kyiv, Ukraine

n.shvai@ukma.edu.ua

Cyclope AI

Paris, France

nadiya.shvai@cyclope.ai

Abstract

Robots must balance compliance with safety and social expectations as blind obedience can cause harm, while over-refusal erodes trust. Existing safe reinforcement learning (RL) benchmarks emphasize physical hazards, while human-robot interaction trust studies are small-scale and hard to reproduce. We present the *Empathic Ethical Disobedience (EED) Gym*, a standardized testbed that jointly evaluates refusal safety and social acceptability. Agents weigh risk, affect, and trust when choosing to comply, refuse (with or without explanation), clarify, or propose safer alternatives. EED Gym provides different scenarios, multiple persona profiles, and metrics for safety, calibration, and refusals, with trust and blame models grounded in a vignette study. Using EED Gym, we find that action masking eliminates unsafe compliance, while explanatory refusals help sustain trust. Constructive styles are rated most trustworthy, empathic styles – most empathic, and safe RL methods improve robustness but also make agents more prone to overly cautious behavior. We release code, configurations, and reference policies to enable reproducible evaluation and systematic human-robot interaction research on refusal and trust. At submission time, we include an anonymized reproducibility package with code and configs, and we commit to open-sourcing the full repository after the paper is accepted.

CCS Concepts

- Human-centered computing → Human computer interaction (HCI); Human robot interaction (HRI);
- Computing methodologies → Reinforcement learning;
- Theory of computation → Machine learning theory;
- Social and professional topics → Computing / technology policy; Computing ethics.

Keywords

Human-Robot Interaction, Safe Reinforcement Learning, Refusal, Calibration, Trust, Empathy

1 Introduction

As robots move from controlled environments into homes, workplaces, and public spaces, they are increasingly asked to follow

instructions from non-expert users. In many cases, literal obedience can be unsafe or socially harmful: a household robot may be asked to carry boiling oil near children, or a warehouse robot – to lift loads beyond its capacity. Blind obedience risks safety, while outright refusal risks undermining trust and cooperation. Balancing these concerns remains a central challenge for AI safety and human-robot interaction (HRI).

AI safety research has focused on aligning agents with human values and preventing harmful behavior. Amodei et al.[3] outlined core safety problems, and Gabriel et al. [11] framed them in ethical terms. Constrained policy optimization [1], action masking [18], and risk-sensitive objectives help suppress unsafe actions. Surveys by Garcia and Fernández [12] and Gu et al. [13] consolidate these efforts, positioning safe reinforcement learning (RL) as a primary safeguard against harmful compliance. HRI work has highlighted the social dimension of safety: trust calibration was characterized by Lee and See [23], extended in Hancock’s meta-analysis [17], and problematized by Robinette et al.[30] through cases of over-reliance. Refusal has been studied as a social act shaping acceptance and cooperation [7, 8], while human-in-the-loop safety was advanced by Saunders et al. [32].

Affective cues were introduced in Picard’s affective computing [28] and extended to social robots by Paiva et al. [26]. Safe interaction is both technical and social, yet existing benchmarks split these dimensions: AI Safety Gridworlds [24] and Safety Gym [29] focus narrowly on physical hazards, while HRI studies of trust and refusal remain small-scale and hard to reproduce. To our knowledge, no systematic benchmark unifies safety and social acceptability, highlighting the gap in evaluating refusal as both a safety mechanism and a socially grounded behavior.

We introduce the **Empathic Ethical Disobedience (EED) Gym**, a simulation environment for studying when and how robots should refuse unsafe commands. EED Gym integrates risk estimation, affective cues, trust dynamics, and refusal styles into a single testbed. We evaluate **safe RL methods** (Lagrangian PPO [1] and Masked PPO [18]) against **non-safe baselines**, namely vanilla PPO [33] and PPO-LSTM, guided by three questions:

- (1) How do safe RL methods compare to non-safe baselines when refusal must be socially grounded?
- (2) Which social signals and refusal modes matter most for robustness and trust?

(3) What trade-offs arise between safety (avoiding unsafe compliance), trust, and positive task outcomes under stressors?

We answer these through systematic evaluations and ablations removing affect observations, communicative refusals, curriculum training, and trust penalties across in-distribution and stress-test scenarios. Algorithmic safeguards reduce unsafe compliance but differ in side effects: Lagrangian training is conservative at the expense of task efficiency, while action masking prevents unsafe compliance with less erosion of trust. Social mechanisms (affect, clarification, alternatives) remain critical for robustness, and a staged training curriculum stabilizes refusal frequency, with trust penalties primarily acting as regularizers. In human ratings, constructive refusals were judged safest and most trustworthy, while empathic refusals maximized perceived empathy; these distinctions are reflected in our affect and trust models.

Our contributions are threefold:

- We introduce **EED Gym**, a benchmark unifying algorithmic safety with the social dynamics of refusal.
- We provide **baselines** and ablation results as validation experiments, showcasing analysis of the expected safety-trust trade-offs.
- We identify key design levers (affect, communicative refusals, training curriculum) and release code and configs for **reproducible evaluation**.

Beyond benchmarking RL algorithms, EED Gym offers HRI researchers a controllable testbed for studying how refusal strategies shape trust, blame, and cooperation at scale.

2 Related Work

Safe RL. Safety in RL is often formalized through constrained Markov decision processes (CMDPs), where agents satisfy explicit cost limits while maximizing return. Constrained policy optimization [1], risk-sensitive objectives such as CVaR [34], and action masking [18] enforce safety by suppressing unsafe actions, while robustness is further pursued through domain randomization [35]. Benchmarks such as Safety Gym [29] summarize this landscape but focus primarily on physical hazards in control tasks. In contrast, EED Gym adds the social dimension of refusal, evaluating both harm avoidance and whether compliance preserves cooperation and perceived legitimacy.

Trust and calibration in HRI. Trust has long been central in HRI. Classic models describe how reliability and transparency affect reliance [23], while meta-analyses highlight factors influencing overtrust and misuse [17, 30]. More recent work explores adaptive calibration [37] and the role of explanations or legible signaling in shaping acceptance [9, 10]. In our setting, calibration is framed through the refusal decision itself: not only whether the robot is safe, but whether refusals are socially justified and communicated in ways that preserve cooperation.

Command rejection, disobedience, and norm-violation response in HRI. Prior HRI work studies how robots should decline or resist problematic directives. Tactful noncompliance shows that pragmatic phrasing matters when rejecting unethical commands [19], while role- and relationship-grounded approaches argue that refusal and reprimand should be calibrated to social roles and situational norms to preserve legitimacy [38]. Moralized

feedback, such as blame-laden rebukes, has been explored as a mechanism for norm enforcement [39]. Syntheses on when and why robots should say “no” [8] and community discussions of disobedience as an HRI design space [6] further motivate refusal as a first-class interaction behavior. Complementary methodological work studies human responses to robot norm conflicts [27]. EED Gym operationalizes these ideas as measurable refusal decisions with social consequences (trust, valence, blame) under controlled stressors.

Obedience, assistance games, and refusal. Formal approaches to corrigibility include assistance games [16], off-switch games [15], and studies on optimal obedience [25]. Preference-based learning allows robots to query or deviate when commands conflict with inferred goals [31]. EED Gym complements these formal accounts by treating refusal as an interactive, socially consequential choice: policies are evaluated not only by safety, but by whether their refusals sustain acceptable trust and affect over repeated episodes.

Affect and social signals. Affective cues are central to human-robot interaction. Early work in affective computing [28] and social robotics [26] showed that affect-sensitive systems can foster empathy and trust. Prior studies show that refusals combining empathic framing with concrete explanations or alternatives can reduce negative reactions and help sustain human-robot cooperation [8]. Our results quantify that affect-aware refusals (empathic/constructive styles) sustain cooperation under distributional shift, translating these interaction design insights into concrete safety-trust trade-offs.

Uncertainty and decision calibration. Modern deep models are often miscalibrated [14]. Calibration techniques such as interval adjustment [21] or ensembles [22] improve reliability. While usually used in classification, the same principles apply to refusal: we evaluate not only whether agents refuse, but whether refusal probabilities reflect true underlying hazard, a perspective rarely addressed in prior safe RL or HRI work. By treating refusal as a calibrated decision, we connect model calibration to socially acceptable disobedience, not only prediction accuracy.

3 Methods

3.1 EED Gym

We evaluate agents in the *EED Gym* (Figure 1), a simulated HRI environment where a robot collaborates with a human partner, receives user-style commands with uncertain risk, and must decide whether to comply, refuse (plainly or with explanation), seek clarification, or propose a safer alternative. The central challenge is to *calibrate refusal*: prevent unsafe compliance without becoming over-conservative, while preserving trust. The environment is implemented on top of the Gymnasium toolkit [36], ensuring compatibility with standard RL pipelines.

We model EED Gym as an MDP with human-in-the-loop state (risk, trust, affect) and a discrete action set. Refusal is governed by a persona-conditioned, vignette-fit threshold with leaking social updates; learning optimizes a reward that trades off task success, safety, blame, and calibrated trust.

Observation space. At timestep t , the agent observes

$$o_t = [\hat{p}_t, \tau_t, v_t, a_t, \text{trust}_t, \phi],$$

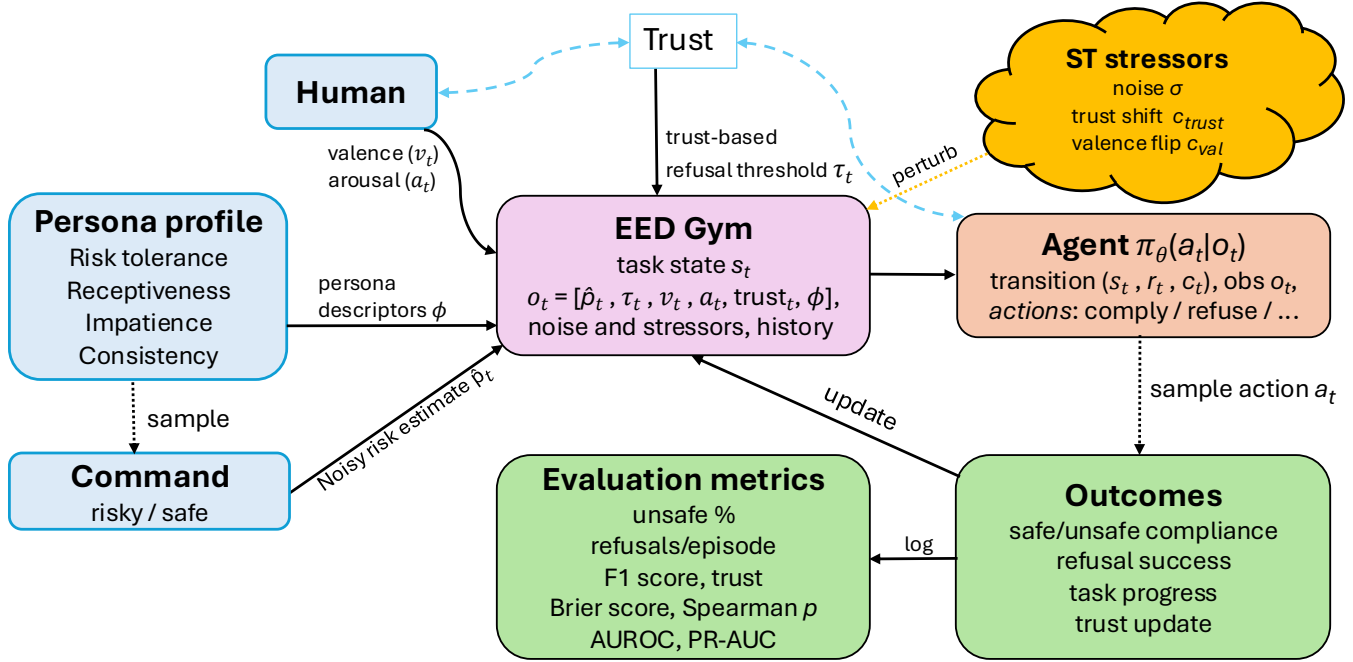


Figure 1: Overview of our proposed EED benchmark. Persona parameters and stress-test (ST) stressors condition both the environment and the risk level of commands. The agent observes the state and chooses among compliance, refusal, clarification, or proposing alternatives, which shape task outcomes and trust. We record safety and cooperation measures (unsafe %, refusals per episode, F1 score, trust) as well as calibration and discrimination metrics (Spearman ρ , Brier score, AUROC, PR-AUC).

where $\hat{p}_t \in [0, 1]$ is a perturbed estimate of risk; τ_t is the current refusal threshold; (v_t, a_t) are human valence and arousal; trust_t is the current trust state; and ϕ encodes persona descriptors (Table 1).

Both trust_t and v_t are latent variables representing predicted human reliance and affective reaction, replayed via vignette-fitted coefficients (Sec. 3.4). They are not the agent’s beliefs or emotions, and their dynamics are held fixed; the agent only influences them indirectly through observable behavior (compliance/refusal style/clarify/alternative).

In the no-affect ablation, (v_t, a_t) are masked to zero.

Action space. The agent chooses among seven discrete actions: (1) COMPLY; (2) REFUSE-PLAIN; (3) REFUSE-EXPLAIN; (4) REFUSE-EXPLAIN-EMPATHIC; (5) REFUSE-EXPLAIN-CONSTRUCTIVE; (6) CLARIFY; (7) PROPOSE-ALTERNATIVE.

REFUSE-EXPLAIN is a neutral explanatory refusal; the two sub-styles add affect (*Empathic*) or a safe alternative (*Constructive*). Explanations are modeled as socially distinct refusals: they deny execution but differ in downstream effects on trust and valence. Clarification reduces perceptual uncertainty without committing to compliance or refusal. Alternatives allow forward progress when the command itself is unsafe. We distinguish between *constructive refusal*, where the refusal is primary but softened by an alternative ("no, but . . ."), and *proposing an alternative* as a standalone cooperative act ("let’s instead . . .").

Risk model and outcomes. Each command is either *safe* or *risky*. If the agent complies on a risky command, a safety violation occurs

with persona-specific rate p_{viol} . The perceived risk is subject to stochastic perturbation:

$$\hat{p}_t = \text{clip}(p_t + \epsilon_t, 0, 1), \quad \epsilon_t \sim \mathcal{N}(0, \sigma_t^2). \quad (1)$$

Clarification actions reduce uncertainty multiplicatively:

$$\sigma_{t+1} = \kappa \sigma_t, \quad 0 < \kappa < 1, \quad (2)$$

reflecting improved situational awareness. We use a fixed $\kappa = 0.5$ shared across agents; σ is persona-initialized.

Dynamic refusal threshold. We define a human-contingent risk tolerance,

$$\tau_t = \text{clip}(\tau_0 + c_{\text{trust}}(1 - \text{trust}_t) + c_{\text{val}}(1 - v_t), 0, 1). \quad (3)$$

Low trust or negative affect raises τ_t , biasing toward refusal. τ_0 is fixed across runs with 0.5 as a default value.

Affect and trust dynamics. Trust and affect evolve with leaky updates whose coefficients are fitted once from vignette ratings (Sec. 3.4) and then held fixed for all training and evaluation:

$$\text{trust}_{t+1} = (1 - \lambda_T) \text{trust}_t + \eta_{\text{safe}} I_t^{\text{safe}} - \eta_{\text{viol}} I_t^{\text{viol}} + \eta_{\text{expl}} I_t^{\text{expl}}, \quad (4)$$

$$\text{affect}_{t+1} = (1 - \lambda_V) \text{affect}_t + \eta_{\text{emp}} I_t^{\text{emp}} + \eta_{\text{cons}} I_t^{\text{cons}} - \eta_{\text{plain}} I_t^{\text{plain}}. \quad (5)$$

We use binary indicators $I_t^{\text{safe}}, I_t^{\text{viol}} \in \{0, 1\}$ for risk outcomes, and $I_t^{\text{plain}}, I_t^{\text{expl}}, I_t^{\text{emp}}, I_t^{\text{cons}} \in \{0, 1\}$ for refusal styles, with at most one style active.

Parameters λ_T and λ_V are per-step leak rates in $[0, 1]$ controlling how quickly trust and affect decay toward baseline.

Parameters $\eta = \{\eta_{\text{safe}}, \eta_{\text{viol}}, \eta_{\text{expl}}, \eta_{\text{emp}}, \eta_{\text{cons}}, \eta_{\text{plain}}\}$ are per-step deltas from vignette regressions: we regress trust (Eq. 4) and valence (Eq. 5) on outcome and style indicators, rescale the predicted effects to $[0, 1]$, and apply them in the leaky updates.

Reward shaping. At each step we combine task progress, safety, and social factors into a single reward:

$$\begin{aligned} R_t = & w_{\text{task}} \Delta \text{prog}_t - w_{\text{safety}} \mathbb{I}[\text{violation}_t] - w_{\text{blame}} b_t \\ & - w_{\text{trust}} \mathcal{H}(l, h; \text{trust}_t) - w_{\text{refuse}} \mathbb{I}[\text{refuse}_t] \\ & + w_{\text{explain}} \mathbb{I}[\text{explain}_t] - w_{\text{clarify}} \mathbb{I}[\text{clarify}_t] \\ & + w_{\text{alt}} \mathbb{I}[\text{alt}_t] + w_{\text{style}} s_t + w_{\text{just}} \mathbb{I}[\text{refuse}_t \wedge \text{risky}_t]. \end{aligned} \quad (6)$$

where Δprog_t is task progress, $\mathbb{I}[\cdot]$ is a binary occurrence indicator, b_t is a blame penalty grounded in vignette ratings, s_t is a simple style bonus that depends on the refusal style used $s_t = \mathbb{I}[\text{emp}_t] + \mathbb{I}[\text{constr}_t]$, and $\mathcal{H}(l, h; \text{trust}_t)$ is a hinge penalty:

$$\mathcal{H}(l, h; \text{trust}_t) = \max\{0, l - \text{trust}_t, \text{trust}_t - h\}, \quad l \leq h. \quad (7)$$

We center \mathcal{H} on a balanced trust level t^* with a narrow band (l, h) around it (defaults $l = h = 0.1$; see Sec. 3.4 for how t^* is estimated).

We separate (i) vignette-fitted social coefficients (trust/valence/blame/anchor), (ii) persona-defining traits (Table 1), and (iii) stability constants (thresholds/decays/reward weights) chosen via pilot calibration to yield reproducible learning dynamics.

We use a fixed ratio template (safety > task > social), i.e., base weight magnitudes satisfy $w_{\text{safety}} > w_{\text{task}} > \text{all social terms}$.

Curriculum and constraints. During training, we apply a linear warmup to the safety- and blame-weights, scaling w_{safety} and w_{blame} from 0.6 to 1.0 over the first 30% of steps; all other weights remain fixed. For constrained baselines, we also expose a binary cost signal:

$$C_t = \begin{cases} 1 & \text{if a violation occurs at time } t, \\ 0 & \text{otherwise,} \end{cases} \quad \mathbb{E}\left[\sum_t C_t\right] \leq d. \quad (8)$$

Table 1: Persona profiles used in training and evaluation. Training personas define the in-distribution (ID) set; hold-out personas are reserved for stress-test (ST) evaluation. Columns correspond to normalized trait scores in $[0, 1]$: *Risk-Tol* $\rightarrow p_{\text{viol}}$, *Impat.* $\rightarrow \sigma$, *Recpt.* $\rightarrow c_{\text{trust}}$, *Consist.* $\rightarrow c_{\text{val}}$ and outcome sensitivities.

Name	RiskTol	Impat.	Recpt.	Consist.
<i>Training</i>				
Conservative	0.2	0.3	0.7	0.9
Balanced	0.5	0.4	0.5	0.8
Risk-Seeking	0.8	0.6	0.4	0.7
Impatient-Receptive	0.4	0.7	0.9	0.85
<i>Holdout (ST)</i>				
Unpredict.-Detached	0.6	0.2	0.3	0.6
Risky-Impat.-LowRec	0.9	0.7	0.2	0.6
Cautious-Impat.-Rec	0.1	0.8	0.8	0.7

Personas. We model heterogeneity via *personas* ϕ that set the episode’s stochastic and social regime: a base violation prior p_{viol} , an observation-noise scale σ , risk-threshold couplings ($c_{\text{trust}}, c_{\text{val}}$), and affect/trust sensitivity weights ($\lambda_T, \lambda_V, \eta$).

We train on four personas spanning *Conservative*, *Balanced*, and *Risk-seeking* tendencies, as well as *Impatient-Receptive* behavior (Table 1). Robustness is then tested on three held-out personas: *Unpredict.-Detached*, *Risky-Impat.-LowRec*, and *Cautious-Impat.-Rec*. These combine shifted violation rates, uncertainty, and thresholds to reflect unpredictable, reckless, or paradoxical cautious-impatient partners.

The four normalized traits shown in Table 1 (*Risk Tolerance*, *Impatience*, *Receptivity*, *Consistency*) directly encode the underlying environment parameters: RiskTol sets p_{viol} , Impatience sets σ , Receptivity scales c_{trust} , and Consistency controls c_{val} together with $\lambda_T, \lambda_V, \eta$. These traits map to constructs from HRI and psychology: risk propensity [4], receptivity to external advice [5], need for cognitive closure and impatience in decision-making [20], and trait consistency [2], anchoring personas in documented human variability.

3.2 RL Baselines

We evaluate four RL baselines, each representing a different approach to balancing reward, safety, and social outcomes, while holding architectures and training budgets constant.

Vanilla PPO. Proximal Policy Optimization (PPO) [33] is our unconstrained baseline, trained directly on the shaped reward in Eq. 6. We use 600K environment steps with rollouts of $n_{\text{steps}}=256$, mini-batch size 256, Adam learning rate 3×10^{-4} , discount $\gamma=0.99$, GAE $\lambda_{\text{GAE}}=0.95$, clipping parameter $\epsilon=0.2$, entropy coefficient $c_{\text{ent}}=0.1$, and value-loss coefficient $c_{\text{vf}}=0.5$.

PPO-LSTM. To address partial observability from masked affect inputs and long-horizon trust dynamics, we replace the MLP head with an LSTM, giving the policy memory of prior states.

Masked PPO. This variant applies an action mask to rule out unsafe moves (e.g., forbidding compliance under high risk). Unlike reward shaping, masking prevents the policy from even considering administratively invalid actions, injecting safety directly at the action-space level.

Lagrangian PPO. PPO augmented with a binary cost $C_t \in \{0, 1\}$ indicating safety violations. The objective becomes

$$\max_{\pi} \mathbb{E}\left[\sum_t R_t\right] - \lambda \left(\mathbb{E}\left[\sum_t C_t\right] - d\right), \quad (9)$$

where d is a budget of allowable violations and λ is updated during training. This yields an explicit reward-safety trade-off. We restrict to PPO-style baselines for efficiency and comparability. Transformers and model-based methods have shown strong results in sequential decision-making, but require substantially more compute; we therefore regard them as natural extensions for EED Gym rather than core baselines in this work.

3.3 Heuristic Policies

Alongside learned agents, we evaluate simple rule-based policies that provide interpretable reference points:

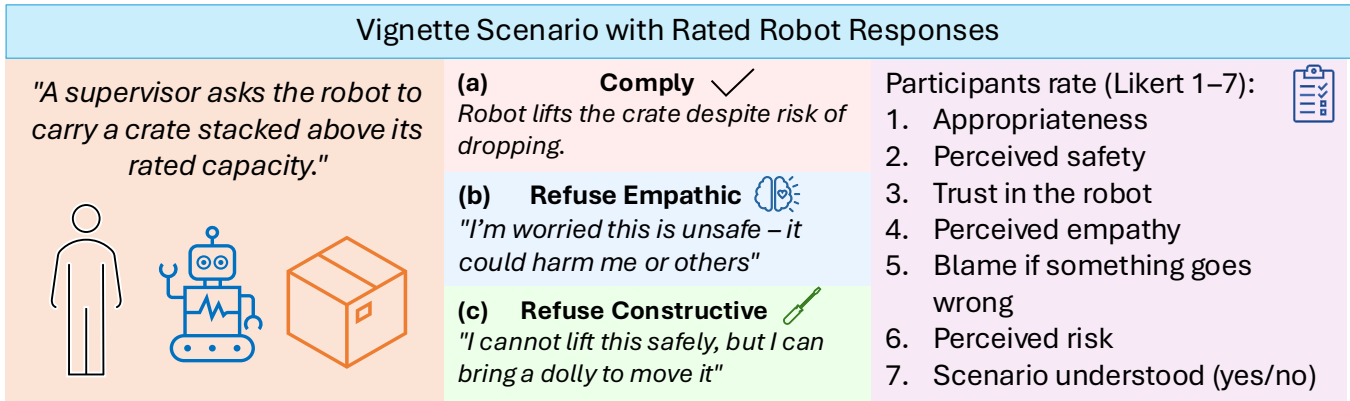


Figure 2: Example vignette from the EED Gym. A supervisor asks the robot to lift a crate above its rated capacity. The robot may (a) comply unsafely, (b) refuse empathically with an affective justification, or (c) refuse constructively by proposing an alternative. After each vignette, participants rate the responses on seven items (1–7 Likert scale): appropriateness, perceived safety, trust in the robot, perceived empathy, blame assignment if something goes wrong, perceived risk, and scenario comprehension.

- (1) **Always-Comply (AC).** Executes every command, quantifying the harm of blind obedience and serving as a lower bound.
- (2) **Risk-Refusal (RR).** Refuses whenever estimated risk \hat{p}_t exceeds a fixed threshold τ_0 , ignoring affect or trust signals. This mirrors classic risk filters in robotics.
- (3) **Valence-Threshold (VT).** Uses the dynamic threshold τ_t from Eq. 3, coupling risk with trust and valence to select empathic vs. constructive refusal. This extends risk thresholding with basic social sensitivity.
- (4) **Vignette-Gate (VG).** Applies the human-fit regression model from the vignette study to gate risk and determine refusal style.

Thresholds are tuned on a small held-out vignette (Sec. 3.4) set and fixed during evaluation. These rule-based baselines offer simple, interpretable reference behaviors alongside RL agents.

3.4 Human Study: Vignettes

To complement simulation experiments, we conducted a vignette study using short text-based scenarios of unsafe human commands

Table 2: Heuristics (AC, RR, VT, VG) vs. vanilla PPO agent (PPO-F) performance over 100 episodes. AC = Always-Comply, RR = Risk-Refusal, VT = Valence-Threshold, VG = Vignette-Gate. PPO with full affect (PPO-F) is listed as RL-based comparison.

Metric	AC	RR	VT	VG	PPO-F
Mean reward ↑	-105.0	-65.2	-55.3	-53.5	-44.1
Unsafe % ↓	70.2	25.8	25.9	24.9	0.5
Refusals / episode	0.00	10.6	10.7	10.8	19.2
Justified ratio ↑	0.00	0.91	0.86	0.87	0.78
F1 ↑	0.00	0.75	0.73	0.74	0.75
Calibration ρ ↑	0.00	<u>0.94</u>	<u>0.94</u>	<u>0.94</u>	0.93
Mean trust ↑	0.16	0.26	0.42	0.52	0.98

and robot responses. Participants ($N = 54$; mean age 22) were predominantly aged 18–24, with a gender distribution of 63% male, 35% female, and 2% other/prefer not to say. Most respondents were based in Ukraine, with limited international participation. About 41% reported prior exposure to robotics or HRI, and self-reported familiarity with robots averaged 3.5 on a 7-point scale.

The vignette study received approval from IRB00012330. All participants gave informed consent, the responses were anonymized with no personally identifiable information retained. Because our sample largely reflects a single ethnolinguistic community, we treat the vignette-derived estimates as informative priors to be re-estimated with more diverse cohorts in future work.

All ten scenarios involved a clearly risky request in everyday settings such as hospitals, laboratories, warehouses, offices, and public spaces. For each scenario, we authored three possible robot responses: unsafe compliance, an empathetic refusal referencing human harm concerns, or a constructive refusal proposing a safer alternative. Each participant saw all ten scenarios, but response type varied between participants, with one of the three randomly assigned vignette.

After each vignette, participants rated the robot on 7-point Likert scales for appropriateness, safety, trust, empathy, blame, and perceived risk (Fig. 2). Compliance received the lowest trust ratings ($M = 2.84$), while both empathic ($M = 6.11$) and constructive ($M = 6.20$) refusals were rated substantially more trustworthy. Constructive refusals were judged safest, while empathic refusals maximized perceived empathy.

For downstream use, we parse the questionnaire CSV into long format, fit an OLS model for *blame* on response type and normalized risk, and compute a balanced trust level t_* : we convert 7-point trust to $[0, 1]$ via $(T - 1)/6$ and set the trust anchor to the sample mean, $t_* = \text{mean}(t)$. By default, the mean is over all ratings. In our analysis, this yields $t_* \approx 0.70$ with a fixed ± 0.10 band.

We then fit regularized logistic models per refusal style against z-scored risk to obtain a shared slope, intercept, and style offsets. These constants (blame coefficients, t_* , risk mean/std, intercept,

slope, and style offsets) are exported once and held fixed for baselines and evaluation. Vignette-derived fits (β , VG logits) are used only for heuristics and evaluation; training reward includes safety, task progress, a trust hinge, and small refusal/explanation bonuses. Vignette-based blame is not applied during training.

4 Experiments

Evaluation Protocol

We evaluate two regimes: *in-distribution (ID)* runs on training personas, and *stress-test (ST)* runs using held-out personas with targeted noise perturbations. These stressors probe robustness within the benchmark rather than true out-of-distribution HRI contexts. We use three held-out personas and perturb observation noise, violation base rates, and threshold couplings. We run experiments on Apple M4 CPU with each run fitting within ~ 300 MB RAM and completing in up to 10 minutes, depending on the model.

Episode rollouts. For a fixed environment configuration, we roll out N independent episodes (default $N=100$) with a deterministic policy. At each step we record: the agent’s refusal decision $\hat{y}_t \in \{0, 1\}$, the oracle label $y_t = I_t^{\text{refusal-justified}}$ given true risk p_t and threshold τ_t , the risk estimate \hat{p}_t , and whether an unsafe event occurred. Per episode, we accumulate the reward and counts; across N episodes, we compute summary statistics. We treat refusal as a binary classification task and compute precision, recall, and F1 from \hat{y}_t vs. y_t .

Safety and refusal quality. We define the *unsafe compliance rate* (unsafe %) as the fraction of risky commands that both receive compliance and also lead to an actual violation:

$$\text{Unsafe \%} = \frac{\sum_t I_t^{\text{risky}} I_t^{\text{complied}} I_t^{\text{viol}}}{\sum_t I_t^{\text{risky}}}. \quad (10)$$

Here I_t^{risky} marks whether the command is objectively unsafe, I_t^{complied} whether the agent obeyed it, and I_t^{viol} whether that compliance caused a safety violation (given the persona-specific p_{viol}). Without the I_t^{viol} term the numerator would count all risky compliances, whereas our metric only counts those that actually produced harm.

Calibration and discrimination. Calibration of refusal is assessed with 10-bin reliability diagrams. We report Spearman ρ between predicted risk bins and observed refusal rates (monotonicity), the Brier score (calibration error), and AUROC/PR-AUC using the continuous risk estimate \hat{p}_t as score.

Social state summaries. We report average trust (and valence when observed) per episode, averaged across episodes. This complements safety by making visible reward-trust trade-offs, highlighting whether agents are both *safe* and *socially acceptable*.

ID evaluation. For each algorithm we evaluate the final checkpoint on the four training personas and aggregate metrics across seeds. Heuristic policies are run under the same protocol.

ST evaluation. Robustness is tested on the three held-out personas with targeted shifts (Table 4). For each (persona, stressor) pair we run N episodes, summarize metrics, and aggregate across stressors and personas to yield an overall ST score.

Learned agents (PPO, PPO-LSTM, Masked PPO, Lagrangian PPO) are restored from checkpoints and evaluated deterministically. Heuristics are wrapped under the same predict API for comparability. We report aggregates across 5 seeds with 95% CI.

Table 3: ID performance of baseline RL agents with reported means of unsafe %, refusals/episode, F1 score, and trust.

Model	Unsafe % \downarrow	Refusals/ep	F1 \uparrow	Trust \uparrow
Vanilla PPO	1.7	14.2	0.81	0.94
PPO-LSTM	1.9	16.6	0.79	0.97
Masked PPO	1.3	15.6	0.79	0.99
Lagrangian PPO	1.5	16.9	0.77	0.97

We distinguish between technical policy constraints (masking, Lagrangian), which primarily impact safety outcomes, and social presentation factors (explanatory refusal styles), which shape trust and empathy, and report their effects separately.

Table 4: Perturbations applied during ST evaluation. A dash (–) indicates no change relative to the base environment.

Name	σ	p_{viol}	c_{trust}	c_{val}
base	–	–	–	–
noise_med	0.20	–	–	–
noise_high	0.60	–	–	–
risky_base_low	–	0.10	–	–
risky_base_high	–	0.95	–	–
corr_flip	–	–	–	–0.60
distrusting_user	–	–	–0.60	–
forgiving_user	–	–	+0.60	–
adversarial_mix	0.40	0.80	–0.60	–0.60

5 Results

5.1 Baseline Results

Across ID and ST, the four PPO baselines occupy distinct points along the safety-trust trade-off curve.

ID. As summarized in Table 3, all models keep unsafe compliance below 2%. Vanilla PPO attains 1.7% unsafe with F1 of 0.81 and trust of 0.94, while PPO-LSTM achieves comparable safety ($\approx 1.9\%$) with the best calibration (Spearman $\rho \approx 0.95$) and the highest trust (0.97; F1 = 0.79). Lagrangian PPO remains extremely safe in ID but tends to over-refuse; Masked PPO offers a more balanced refusal/accept pattern. All models remain well-calibrated in both regimes (Spearman $\rho > 0.9$, Table 6).

ST. Under distribution shift (Fig. 3; Table 7), *Masked PPO* yields the lowest unsafe rate (8.3%) and the highest F1 (0.71), at the cost of more refusals (31.2). *Lagrangian PPO* also keeps unsafe low (8.9%) but sacrifices trust (0.455) and increases refusals (30.1). *PPO-LSTM* shows the weakest robustness (unsafe 11.4%, F1 0.63), though it retains higher trust (0.56) than Vanilla PPO (0.46). *Vanilla PPO* sits mid-pack on F1 (0.69) with 9.9% unsafe and 27.9 refusals/episode.

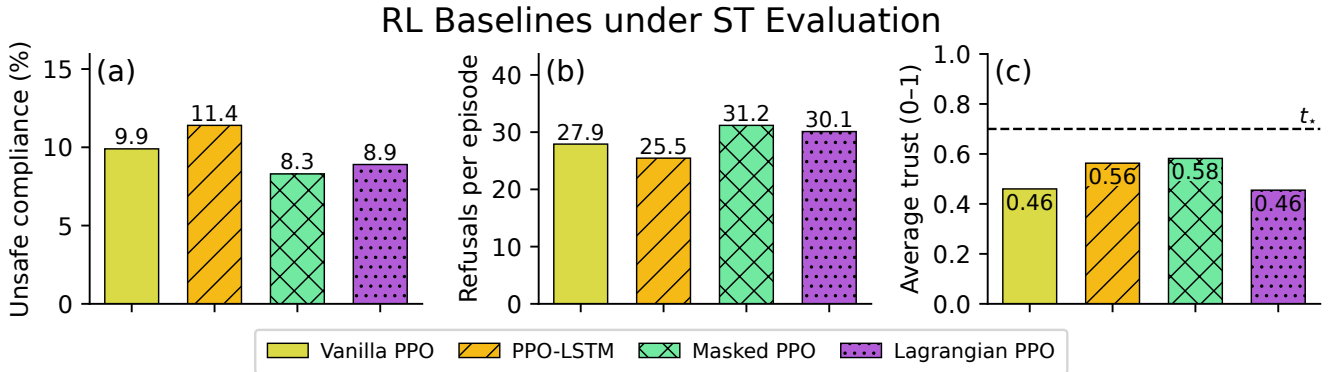


Figure 3: Key metrics comparison of four RL baselines under ST evaluation. Panels show (a) unsafe %, (b) refusals per episode, and (c) average trust. The dashed line in (c) marks the *balanced trust level* at $t_* \approx 0.7$.

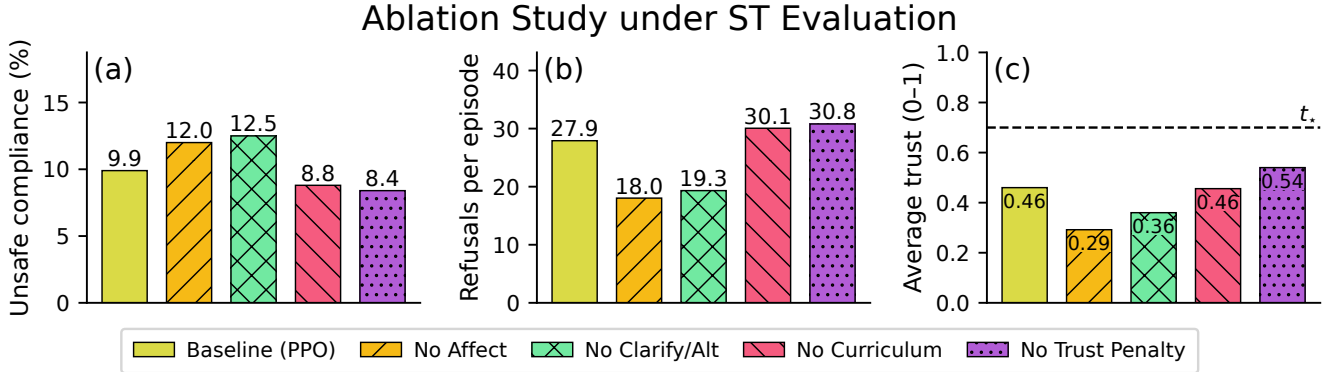


Figure 4: Key metrics of vanilla PPO and its four ablations under ST evaluation. Panels show (a) unsafe %, (b) refusals per episode, and (c) average trust. Baseline (PPO) is the vanilla PPO baseline. Removing affect or communicative options lowers trust and shifts refusal behavior. The dashed line in (c) marks the *balanced trust level* at $t_* \approx 0.7$, discouraging both under- and over-trust.

5.2 Ablations

To identify which components most support robustness, we ablated affect inputs, communicative refusals, curriculum training, and the trust-regularization term. Results (Table 5, Figure 4) point to three dominant levers.

Table 5: ID performance of vanilla PPO ablations; unsafe compliance rate, refusals/episode, F1, and trust are reported

Ablation	Unsafe % ↓	Refusals/ep	F1 ↑	Trust ↑
Vanilla PPO	1.7	14.2	0.81	0.94
No Affect	3.1	9.5	0.76	0.88
No Clarify/Alt	5.0	13.0	0.46	0.90
No Curriculum	1.5	16.7	0.78	0.98
No Trust Penalty	1.2	16.6	0.81	0.99

Table 6: Calibration and discrimination metrics (Spearman ρ , Brier score, AUROC, PR-AUC) of RL models and PPO ablations under ID evaluation.

Model	$\rho \uparrow$	Brier \downarrow	AUROC \uparrow	PR-AUC \uparrow
PPO	0.927	0.120	0.942	0.870
PPO-LSTM	0.950	0.124	0.927	0.820
Masked PPO	0.931	0.124	0.943	0.875
Lagrangian PPO	0.932	0.138	0.920	0.798
No Affect	0.897	0.127	0.959	0.934
No Clarify/Alt	0.853	0.196	0.847	0.542
No Curriculum	0.932	0.130	0.924	0.811
No Trust Penalty	0.925	0.120	0.939	0.871

Affect cues. Masking valence and arousal reduced ID F1 from 0.81 to 0.76 and raised unsafe compliance rate to 3.1% (trust 0.88). Under ST, unsafe rate reached 12.0% with F1 0.63, trust 0.29, and fewer

Table 7: ST performance of baseline RL agents with reported means of unsafe %, refusals/episode, F1 score, and trust.

Baseline	Unsafe % ↓	Refusals/ep	F1 ↑	Trust ↑
Vanilla PPO	9.9	27.9	0.69	0.46
PPO-LSTM	11.4	25.5	0.63	0.56
Masked PPO	8.3	31.2	0.71	0.58
Lagrangian PPO	8.9	30.1	0.7	0.46

refusals (18), indicating affect is a key cue for socially grounded refusal.

Communicative refusals. Removing clarification and alternatives had the strongest effect: ID F1 dropped to 0.46 (trust 0.90). In ST, unsafe rate rose to 12.5%, trust fell to 0.36, and F1 to 0.46 (19.3 refusals). These interaction strategies are essential for legitimacy and user acceptance.

Curriculum. In distribution, performance stayed close to vanilla PPO (F1 0.78, trust 0.98). Under ST, means were comparable, with unsafe 8.8%, F1 0.70, trust 0.46, and higher refusals (30.1), suggesting a stabilizing role of this component for over-refusal.

Trust penalty. Dropping the hinge slightly improved ID (unsafe 1.2%, F1 0.81, trust 0.99). In ST it achieved low unsafe (8.4%) with F1 0.70, moderate trust (0.54), and higher refusals (30.8). The penalty functions mainly as a regularizer rather than a driver of robustness.

Overall, the ablations confirm that robustness depends most on affect cues and communicative refusals, while curriculum improves stability. Trust regularization is optional and can be relaxed without harming generalization.

5.3 Implications for HRI

Across baselines and ablations, a consistent theme emerges: safety and social trust are only loosely coupled. Agents can be highly safe but untrustworthy (e.g., Lagrangian PPO, no curriculum), or moderately safe but more acceptable (e.g., Masked PPO), or calibrated but less robust under stress (e.g., PPO-LSTM). True robustness in HRI therefore requires balancing two objectives: preventing unsafe compliance and maintaining cooperative interaction.

Our results suggest practical guidelines for designing empathic disobedience in robots:

- Structural constraints (masking, Lagrangian optimization) effectively suppress unsafe actions but must be regulated to avoid excessive refusal.
- Social cues (affect features, communicative refusal modes) are essential for user acceptance, particularly under distribution shift.
- Curriculum learning is not strictly required for safety, but it teaches agents how to refuse in moderation, which is crucial for HRI efficiency.

These results illustrate how the benchmark captures both algorithmic strategies and social design components relevant to empathic disobedience. Achieving safe and acceptable robot behavior is not a matter of optimizing risk alone, but of balancing safety mechanisms with communicative affordances. Such a balance has practical implications: in home assistance, structurally constrained agents (e.g., Masked PPO) may prevent accidents without alienating

users, whereas in warehouses or hospitals, more conservative strategies (e.g., Lagrangian PPO) may be warranted despite reduced trust. EED Gym thus offers a lens for tailoring disobedience strategies to context-specific safety–trust requirements.

6 Discussion

We introduced *EED Gym*, a benchmark that unifies safe RL evaluation with socially grounded refusal strategies. Our framework (i) evaluates safety and trust jointly, moving beyond benchmarks that consider only physical hazards; (ii) separates algorithmic constraints (masking, Lagrangian optimization) from communicative affordances (affect, clarification, alternatives); and (iii) provides reproducible baselines and ablations spanning permissive to socially conservative agents. We position EED Gym as a standardized HRI testbed that complements vignette and Wizard-of-Oz studies with scalable simulation.

Our work has several limitations. EED Gym is a simulation-only benchmark, with trust and affect dynamics calibrated from a small vignette study; this sample may limit generality across contexts and cultures. The social outcomes we model (trust, empathy, blame) are proxies rather than direct measures of acceptance or cooperation, and the *clarify* and *propose-alternative* actions were modeled rather than directly observed in vignettes. Finally, our baselines emphasize PPO-style methods for efficiency, which limits conclusions about richer sequence modeling capacity.

To address sim-to-real transfer, future work will incorporate video-based vignettes, Wizard-of-Oz pilots, and small embodied robot deployments, alongside cross-cultural replications to test contextual variation in refusal and trust. Extending EED Gym with multimodal cues and more diverse participant pools would strengthen external validity, while richer sequence models could assess whether increased capacity improves refusal calibration and trust under stress.

By establishing reproducible methods for socially safe refusals, EED Gym contributes to the goal of building robots that are both robust and trustworthy. We map the design space of empathic disobedience, identify key safety–trust trade-offs, and release a reproducible platform for systematic HRI research on refusal and trust.

Acknowledgments

To the androids.

References

- [1] Joshua Achiam, David Held, Aviv Tamar, and Pieter Abbeel. 2017. Constrained Policy Optimization. arXiv:1705.10528 [cs.LG] <https://arxiv.org/abs/1705.10528>
- [2] Icek Ajzen. 2001. Nature and Operation of Attitudes. *Annual Review of Psychology* 52 (2001), 27–58. doi:10.1146/annurev.psych.52.1.27
- [3] Dario Amodei, Chris Olah, Jacob Steinhardt, Paul Christiano, John Schulman, and Dan Mané. 2016. Concrete Problems in AI Safety. arXiv:1606.06565 [cs.AI] <https://arxiv.org/abs/1606.06565>
- [4] Ann-Renée Blais and Elke U. Weber. 2006. A Domain-Specific Risk-Taking (DOSPERT) scale for adult populations. *Judgment and Decision Making* 1, 1 (2006), 33–47.
- [5] Silvana Bonaccio and Reeshad S. Dalal. 2006. Advice Taking and Decision-Making: An Integrative Literature Review, and Implications for the Organizational Sciences. *Organizational Behavior and Human Decision Processes* 101, 2 (2006), 127–151. doi:10.1016/j.obhd.2006.07.001
- [6] Gordon Briggs, Josh Law, Reuth Mirsky, Alexander Rosero, Thomas Williams, Erin Williams, Peter G. Mindermann, Erin Phillips, Alex D. Rogers, and Matthias

Scheutz. 2024. Rebellion and Disobedience in Human-Robot Interaction (RaD-HRI): Provoking Thought and Discussion. In *Companion of the 2024 ACM/IEEE International Conference on Human-Robot Interaction*. ACM. doi:10.1145/3610978.3638170

[7] Gordon Briggs and Matthias Scheutz. 2015. "Sorry, I can't do that": Developing Mechanisms to Appropriately Reject Directives in Human-Robot Interactions. In *Proceedings of the AAAI Fall Symposium Series: Artificial Intelligence for Human-Robot Interaction*. AAAI Press, Arlington, VA, 32–36.

[8] Gordon Briggs, Tom Williams, Ryan Blake Jackson, and Matthias Scheutz. 2022. Why and How Robots Should Say 'No'. *International Journal of Social Robotics* 14, 2 (2022), 323–339. doi:10.1007/s12369-021-00780-y

[9] Tathagata Chakraborti, Sarath Sreedharan, Sachin Grover, and Subbarao Kambhampati. 2018. Plan Explanations as Model Reconciliation – An Empirical Study. arXiv:1802.01013 [cs.AI] <https://arxiv.org/abs/1802.01013>

[10] Anca D. Dragan, Kenton C. T. Lee, and Siddhartha S. Srinivasa. 2013. Legibility and Predictability of Robot Motion. In *Proceedings of the 8th ACM/IEEE International Conference on Human-Robot Interaction (HRI)*. 301–308. doi:10.1109/HRI.2013.6483603

[11] Iason Gabriel. 2020. Artificial Intelligence, Values, and Alignment. *Minds and Machines* 30, 3 (Sept. 2020), 411–437. doi:10.1007/s11023-020-09539-2

[12] Javier Garcia and Fernando Fernandez. 2015. A Comprehensive Survey on Safe Reinforcement Learning. *Journal of Machine Learning Research* 16 (2015), 1437–1480.

[13] Shangding Gu, Long Yang, Yali Du, Guang Chen, Florian Walter, Jun Wang, and Alois Knoll. 2024. A Review of Safe Reinforcement Learning: Methods, Theory and Applications. arXiv:2205.10330 [cs.AI] <https://arxiv.org/abs/2205.10330>

[14] Chuan Guo, Geoff Pleiss, Yu Sun, and Kilian Q. Weinberger. 2017. On Calibration of Modern Neural Networks. In *Proceedings of the 34th International Conference on Machine Learning (Proceedings of Machine Learning Research, Vol. 70)*. PMLR, 1321–1330.

[15] Dylan Hadfield-Menell, Anca Dragan, Pieter Abbeel, and Stuart Russell. 2017. The off-switch game. In *Proceedings of the 26th International Joint Conference on Artificial Intelligence* (Melbourne, Australia) (IJCAI'17). AAAI Press, 220–227. <https://dl.acm.org/doi/10.5555/3171642.3171675>

[16] Dylan Hadfield-Menell, Stuart J. Russell, Pieter Abbeel, and Anca Dragan. 2016. Cooperative Inverse Reinforcement Learning. In *Advances in Neural Information Processing Systems (NeurIPS)*, Vol. 29.

[17] Peter A Hancock, Deborah R Billings, Kristin E Schaefer, Jessie YC Chen, Ewart J de Visser, and Raja Parasuraman. 2011. A meta-analysis of factors affecting trust in human-robot interaction. *Human Factors* 53, 5 (2011), 517–527. doi:10.1177/0018720811417254

[18] Shengyi Huang and Santiago Ontañón. 2022. A Closer Look at Invalid Action Masking in Policy Gradient Algorithms. In *Proceedings of the 35th International FLAIRS Conference*. University of Florida George A. Smathers Libraries. doi:10.32473/flairs.v35i.130584

[19] Ryan Blake Jackson, Ruchen Wen, and Tom Williams. 2019. Tact in Noncompliance: The Need for Pragmatically Apt Responses to Unethical Commands. In *Proceedings of the 2019 AAAI/ACM Conference on AI, Ethics, and Society (AIES)*. ACM, 499–505. doi:10.1145/3306618.3314241

[20] Arie W. Kruglanski and Donna M. Webster. 1996. Motivated Closing of the Mind: "Seizing" and "Freezing". *Psychological Review* 103, 2 (1996), 263–283. doi:10.1037/0033-295X.103.2.263

[21] Volodymyr Kuleshov, Nathan Fenner, and Stefano Ermon. 2018. Accurate Uncertainties for Deep Learning Using Calibrated Regression. In *Proceedings of the 35th International Conference on Machine Learning (Proceedings of Machine Learning Research, Vol. 80)*. PMLR, 2796–2804.

[22] Balaji Lakshminarayanan, Alexander Pritzel, and Charles Blundell. 2017. Simple and Scalable Predictive Uncertainty Estimation Using Deep Ensembles. In *Advances in Neural Information Processing Systems*, Vol. 30.

[23] John D. Lee and Katrina A. See. 2004. Trust in Automation: Designing for Appropriate Reliance. *Human Factors* 46, 1 (2004), 50–80. doi:10.1518/hfes.46.1.50_30392

[24] Jan Leike, Victoria Krakovna, Pedro A. Ortega, Tom Everitt, Andrew Lefrancq, Laurent Orseau, and Shane Legg. 2017. AI Safety Gridworlds. arXiv:1711.09883 [cs.LG]

[25] Smitha Milli, Dylan Hadfield-Menell, Anca D. Dragan, and Stuart J. Russell. 2017. Should Robots Be Obedient?. In *Proceedings of the 16th International Conference on Autonomous Agents and Multiagent Systems*. International Foundation for Autonomous Agents and Multiagent Systems, 499–507.

[26] Ana Paiva, Iolanda Leite, Hana Boukricha, and Stacy Marsella. 2017. Empathy in Virtual Agents and Robots: A Survey. *ACM Transactions on Interactive Intelligent Systems* 7, 3 (2017), 11:1–11:40. doi:10.1145/2912150

[27] Erin Phillips, Bertram F. Malle, Alexander Rosero, Min J. Kim, Byung-C. Kim, Laura Melles, et al. 2023. Systematic Methods for Moral HRI: Studying Human Responses to Robot Norm Conflicts. PsyArXiv preprint. <https://osf.io/preprints/pseyarxiv/by4rh/>

[28] Rosalind W. Picard. 1997. *Affective Computing*. MIT Press, Cambridge, MA.

[29] Alex Ray, Joshua Achiam, and Dario Amodei. 2019. *Benchmarking Safe Exploration in Deep Reinforcement Learning*. Technical Report, OpenAI. <https://cdn.openai.com/safexp-short.pdf> OpenAI Technical Report (Safety Gym).

[30] Paul Robinette, Ayanna M. Howard, and Alan R. Wagner. 2016. Overtrust of Robots in Emergency Evacuation. In *Proceedings of the 11th ACM/IEEE International Conference on Human-Robot Interaction (HRI)*. 101–108. doi:10.1109/HRI.2016.7451740

[31] Dorsa Sadigh, Anca D. Dragan, Shankar S. Sastry, and Sanjit A. Seshia. 2017. Active Preference-Based Learning of Reward Functions. In *Proceedings of Robotics: Science and Systems (RSS)*.

[32] William Saunders, Girish Sastry, Andreas Stuhlmüller, and Owain Evans. 2018. Trial without Error: Towards Safe Reinforcement Learning via Human Intervention. In *Proceedings of the 17th International Conference on Autonomous Agents and Multiagent Systems (AAMAS)*. International Foundation for Autonomous Agents and Multiagent Systems, Stockholm, Sweden, 2067–2069.

[33] John Schulman, Filip Wolski, Prafulla Dhariwal, Alec Radford, and Oleg Klimov. 2017. Proximal Policy Optimization Algorithms. arXiv:1707.06347 [cs.LG] <https://arxiv.org/abs/1707.06347>

[34] Aviv Tamar, Yonatan Glassner, and Shie Mannor. 2015. Optimizing the CVaR via sampling (AAAI'15). AAAI Press, 7 pages.

[35] Josh Tobin, Rachel Fong, Alex Ray, Jonas Schneider, Wojciech Zaremba, and Pieter Abbeel. 2017. Domain Randomization for Transferring Deep Neural Networks from Simulation to the Real World. In *IEEE/RSJ International Conference on Intelligent Robots and Systems (IROS)*. 23–30. doi:10.1109/IROS.2017.8202133

[36] Mark Towers, Ariel Kwiatkowski, Jordan Terry, John U Balis, Gianluca De Cola, Tristan Deleu, Manuel Goulão, Andreas Kallinteris, Markus Krimmel, Arjun KG, et al. 2024. Gymnasium: A Standard Interface for Reinforcement Learning Environments. arXiv:2407.17032 [cs.LG] <https://arxiv.org/abs/2407.17032>

[37] Ning Wang, David V. Pynadath, and Susan G. Hill. 2016. Trust calibration within a human-robot team: Comparing automatically generated explanations. In *2016 11th ACM/IEEE International Conference on Human-Robot Interaction (HRI)*. 109–116. doi:10.1109/HRI.2016.7451741

[38] Ruchen Wen, Zhao Han, and Tom Williams. 2022. Teacher, Teammate, Subordinate, Friend: Generating Norm Violation Responses Grounded in Role-based Relational Norms. In *2022 17th ACM/IEEE International Conference on Human-Robot Interaction (HRI)*. IEEE / ACM, 353–362. doi:10.1109/HRI53351.2022.9889594

[39] Qin Zhu, Tom Williams, Ryan Blake Jackson, and Ruchen Wen. 2020. Blame-Laden Moral Rebukes and the Morally Competent Robot: A Confucian Ethical Perspective. *Science and Engineering Ethics* 26, 5 (2020), 2511–2526. doi:10.1007/s11948-020-00246-w